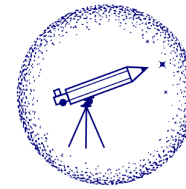


Institute of
Space Sciences



Some usually overlooked aspects in radiative and morphological modelling of pulsar wind nebulae

Diego F. Torres



**MULTIMESSENGER
ASTROPHYSICS**

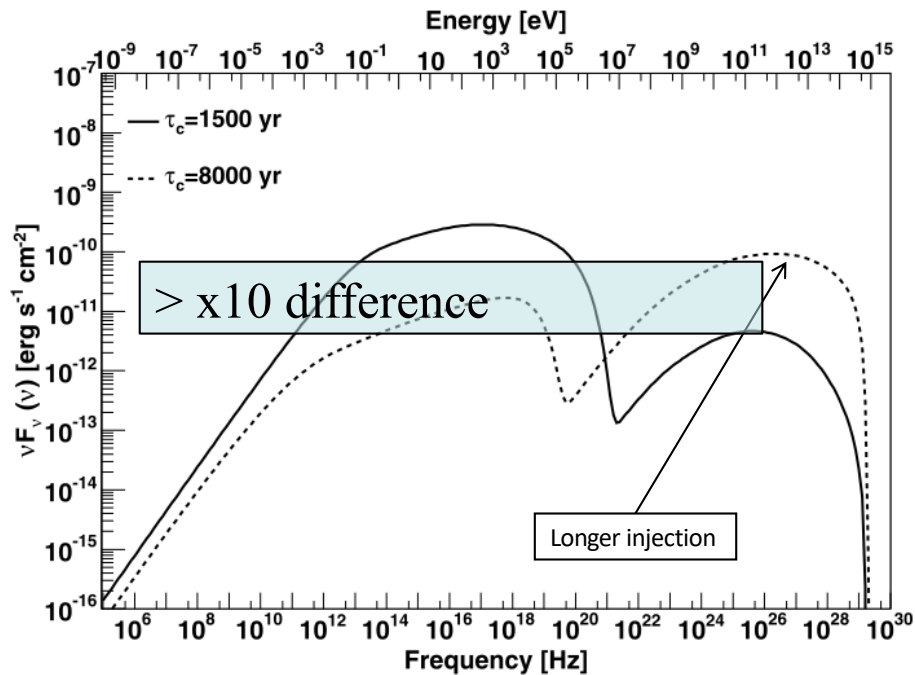
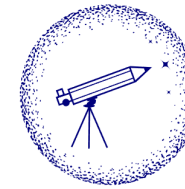
COSMIC RAYS - COMPACT OBJECTS - RELATIVISTIC ENVIRONMENTS

© THE INSTITUTE OF SPACE SCIENCES (ICE, CSIC) SINCE 2006

Starting easy:
 L_{sd}/D^2 is not (in general) a good
estimator of detection likelihood

Spin-down does not tell the whole story

An example



These are PWN spectra from pulsars with the same

- spin-down evolution,
 - spin-down power ($1.7 \times 10^{37} \text{ erg s}^{-1}$)
 - magnetic fraction,
 - injection spectrum,
 - photon background parameters than Crab,
- but two different characteristic ages of 1500 and 8000 years.

Thus, today, B field and PWN size (which depend on evolution) are different and even if the high energy particles have limited life, they are subject to different losses producing different PWN SEDs.

Detectability estimations based on spin-down power (or spin-down power/ D^2) are naive; history counts.

Crab is not so energetically special

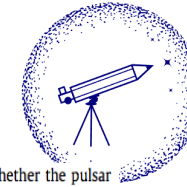


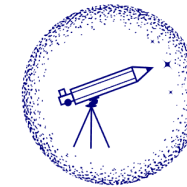
Table from Torres et al. 2014

Pulsars in the ATNF catalog with known period P , and period derivative \dot{P} , and less than 10000 years of characteristic age (τ). The first few columns are taken from ATNF data. The column "TeV Obs.?" answers whether the pulsar has been observed in TeV range, and, if so, by which telescope (noting H for H.E.S.S., M for MAGIC, and V for VERITAS). The column "TeV source" indicates whether there has been a detection of a PWN or in general a TeV source spatially co-located with the pulsar. This information comes from published literature. The last three columns represent, respectively, the age of Crab (assuming today's braking index) at which it would have the same characteristic age than the corresponding pulsar (τ_{sd}^{Crab}), the Crab's spin-down power at that age ($L_{sd}^{Crab}(\tau_{sd}^{Crab})$), and the spin-down power of the pulsar in terms of percentage of $L_{sd}^{Crab}(\tau_{sd}^{Crab})$, which we refer to as CFP (Crab fractional power). Sources noted with † are magnetars, which low rotational power is not expected to contribute significantly to the corresponding TeV sources (marked in red). Names of the TeV sources shown in blue are the ones studied in this work.

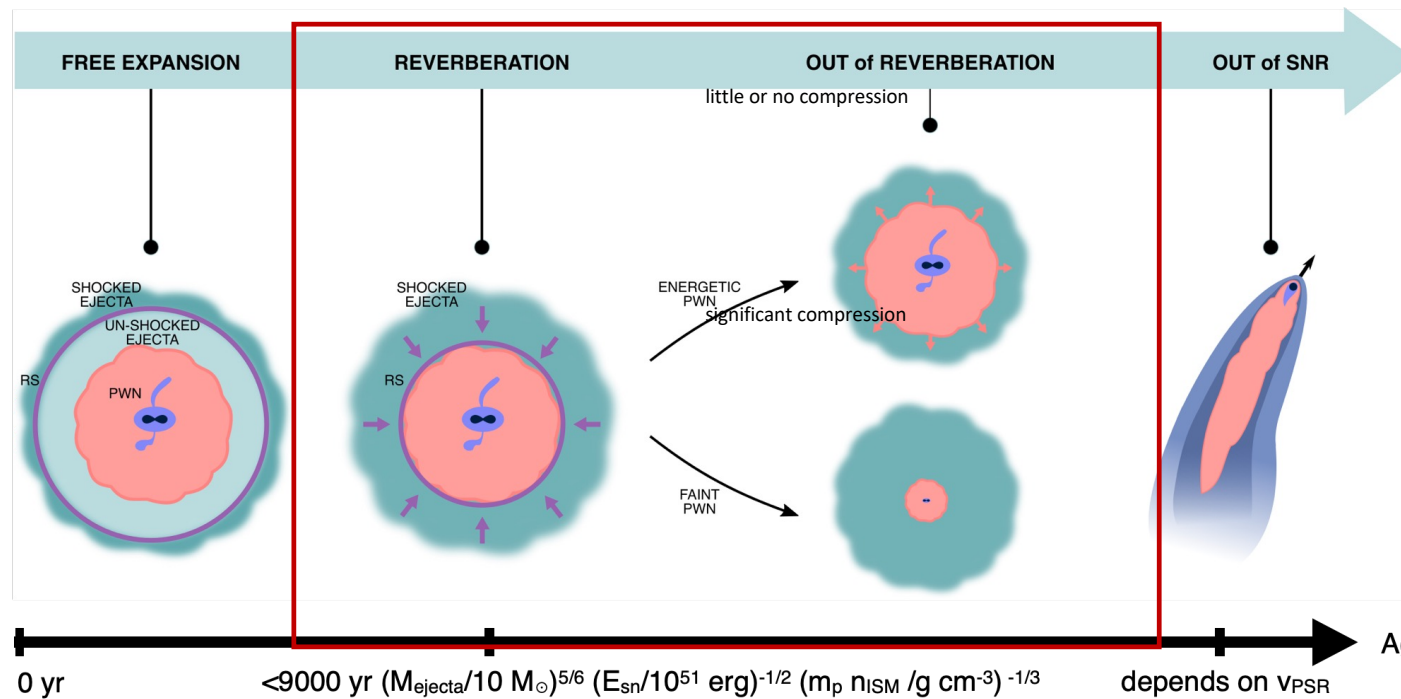
Name	P (s)	\dot{P} ($s s^{-1}$)	D (kpc)	τ (yr)	B_d (G)	L_{sd} ($erg s^{-1}$)	L_{sd}/D^2 ($erg s^{-1} kpc^{-2}$)	TeV Obs.?	TeV source	τ_{sd}^{Crab} (yr)	$L_{sd}^{Crab}(\tau_{sd}^{Crab})$ ($erg s^{-1}$)	CFP (%)
1808–2024†	7.5559	5.49×10^{-10}	13.0	218	2.0×10^{15}	5.0×10^{34}	3.0×10^{32}	H	J1809–194/G11.0+0.08
1846–0258	0.3265	7.10×10^{-12}	5.8	728	4.9×10^{13}	8.1×10^{36}	2.4×10^{35}	H	Kes 75	238	1.6×10^{39}	0.5
1907+0919†	5.1983	9.20×10^{-11}	...	895	7.0×10^{14}	2.6×10^{34}	...	H	J1908+063/G40.1–0.89	459	1.0×10^{39}	0.003
1714–3810†	3.8249	5.88×10^{-11}	...	1030	4.8×10^{14}	4.1×10^{34}	...	H	J1718–385/CTB37A	638	7.2×10^{38}	0.006
0534+2200	0.0334	4.21×10^{-13}	2.0	1258	3.8×10^{12}	4.5×10^{38}	1.2×10^{38}	HMV	Crab nebula	940	4.5×10^{38}	100
1550–5418	2.0698	2.32×10^{-11}	9.7	1410	2.2×10^{14}	1.0×10^{35}	1.1×10^{33}	H	...	1141	3.5×10^{38}	0.03
1513–5908	0.1512	1.53×10^{-12}	4.4	1560	1.5×10^{13}	1.7×10^{37}	9.0×10^{35}	H	J1514–281/MSH 15–52	1340	2.8×10^{38}	6
1119–6127	0.4079	4.02×10^{-12}	8.4	1610	4.1×10^{13}	2.3×10^{36}	3.3×10^{34}	H	J1119–6127/G292.1–0.54	1406	2.6×10^{38}	0.9
0540–6919	0.0504	4.79×10^{-13}	53.7	1670	5.0×10^{12}	1.5×10^{38}	5.1×10^{34}	H	...	1486	2.4×10^{38}	63
0525–6607	8.0470	6.50×10^{-11}	...	1960	7.3×10^{14}	4.9×10^{33}	1871	1.6×10^{38}	0.003
1048–5937	6.4520	3.81×10^{-11}	9.0	2680	5.0×10^{14}	5.6×10^{33}	6.9×10^{31}	H	...	2825	7.8×10^{37}	0.007
1124–5916	0.1354	7.52×10^{-13}	5.0	2850	1.0×10^{13}	1.2×10^{37}	4.8×10^{35}	H	...	3050	6.8×10^{37}	18
1930+1852	0.1368	7.50×10^{-13}	7.0	2890	1.0×10^{13}	1.2×10^{37}	2.4×10^{35}	V	J1930+188/G54.1+0.3	3103	6.6×10^{37}	18
1622–4950	4.3261	1.70×10^{-11}	9.1	4030	2.7×10^{14}	8.3×10^{33}	9.9×10^{31}	H	...	4614	3.0×10^{37}	0.03
1841–0456	11.7789	4.47×10^{-11}	9.6	4180	7.3×10^{14}	1.1×10^{33}	1.2×10^{31}	H	...	4813	2.8×10^{37}	0.004
1023–5746	0.1115	3.84×10^{-13}	8.0	4600	6.6×10^{12}	1.1×10^{37}	1.7×10^{35}	H	J1023+575	5370	2.2×10^{37}	50
1833–1034	0.0618	2.02×10^{-13}	4.10	4850	3.6×10^{12}	3.4×10^{37}	2.0×10^{36}	H	J1833–105/G215–0.9	5701	2.0×10^{37}	170
1838–0537	0.1457	4.72×10^{-13}	...	4890	8.4×10^{12}	6.0×10^{36}	...	H	J1841–055	5754	1.9×10^{37}	32
0537–6910	0.0161	5.18×10^{-14}	53.7	4930	9.2×10^{11}	4.9×10^{38}	1.7×10^{35}	H	N157B (in the LMC)	5807	1.9×10^{37}	2579
1834–0845†	2.4823	7.96×10^{-12}	...	4940	1.4×10^{14}	2.1×10^{34}	...	H	J1834–087/W41	5820	1.9×10^{37}	0.1
1747–2800	0.0521	1.55×10^{-13}	17.5	5310	2.9×10^{12}	4.3×10^{37}	1.4×10^{35}	H	J1747–281/G0.9+0.1	6311	1.6×10^{37}	269
0205+6449	0.0657	1.94×10^{-13}	3.2	5370	3.6×10^{12}	2.7×10^{37}	2.6×10^{36}	MV	...	6390	1.6×10^{37}	169
181											10^{37}	400
010											10^{36}	0.02
135											10^{36}	41
161											10^{36}	22
173											10^{36}	0.9
1617–5055	0.0693	1.35×10^{-13}	6.4	8130	3.1×10^{12}	1.6×10^{37}	3.8×10^{35}	H	J1616–508	10048	5.9×10^{36}	271
2022+3842	0.0242	4.32×10^{-14}	10.0	8910	1.0×10^{12}	1.2×10^{38}	1.2×10^{36}	11082	4.8×10^{36}	2500
1708–4009†	11.0013	1.93×10^{-11}	3.8	9010	4.7×10^{14}	5.7×10^{32}	4.0×10^{31}	H	J1708–443/G343.1–2.69	11215	4.7×10^{36}	0.01
1745–2900†	3.76356	6.5×10^{-12}	8.0	9170	1.6×10^{14}	4.8×10^{33}	7.5×10^{31}	HM	(in the Galactic Center)	11427	4.4×10^{36}	0.99

When Crab has ~6400 years, it would have the same characteristic age than that 3C58 has today, and its luminosity would be almost a factor of 2 lower.

The PWN phases



Plot from Olmi & Bucciantini 2023

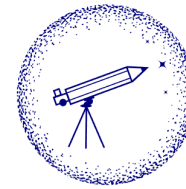


Free expansion proceeds until the PWN reaches the reverse shock (RS).

After that time, the shell experiences a strong deceleration, which in many cases leads to a compression of the PWN.

When due to compression the PWN internal pressure becomes high enough, the PWN bounces and re-expands again.

Reverberation (compression - bounce) last for a few kyrs or less, and happens relatively shortly after birth - at the end of free expansion.



**MULTIMESSENGER
ASTROPHYSICS**

COSMIC RAYS - COMPACT OBJECTS - RELATIVISTIC ENVIRONMENTS

© THE INSTITUTE OF SPACE SCIENCES (ICE, CSIC) SINCE 2006

Then, knowing the shock positions is key

Knowing the shock positions

Bandiera, Bucciantini, Martin, Olmi & DFT, MNRAS 2021

Truelove and McKee (1999, TM99) solutions were used in all models when incorporating the dynamics in radiative models of pulsar wind nebulae (PWNe).

Through a mix of analytical limits, semi-analytical formulae, and fits to numerical simulations, TM99 provides a series of approximations to describe the evolution of the SNR during its different stages.

TM99 has become a widely used reference for the time evolution of the FS and RS.

Scalings

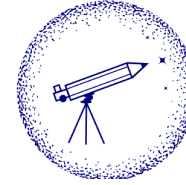
$$R_{\text{ch}} = M_{\text{ej}}^{1/3} \rho_0^{-1/3} \simeq 7.4 \text{ pc} \left(\frac{M_{\text{ej}}}{10 M_{\odot}} \right)^{1/3} \left(\frac{m_{\text{p}} n_0}{\text{g cm}^{-3}} \right)^{-1/3},$$

$$t_{\text{ch}} = E_{\text{sn}}^{-1/2} M_{\text{ej}}^{5/6} \rho_0^{-1/3} \simeq 3241 \text{ yr} \left(\frac{E_{\text{sn}}}{10^{51} \text{ erg}} \right)^{-1/2} \left(\frac{M_{\text{ej}}}{10 M_{\odot}} \right)^{5/6} \left(\frac{m_{\text{p}} n_0}{\text{g cm}^{-3}} \right)^{-1/3}$$

$$V_{\text{ch}} = \frac{E_{\text{sn}}^{1/2}}{M_{\text{ej}}^{1/2}} \simeq 2240 \text{ km s}^{-1} \left(\frac{E_{\text{sn}}}{10^{51} \text{ erg}} \right)^{1/2} \left(\frac{M_{\text{ej}}}{10 M_{\odot}} \right)^{-1/2}$$

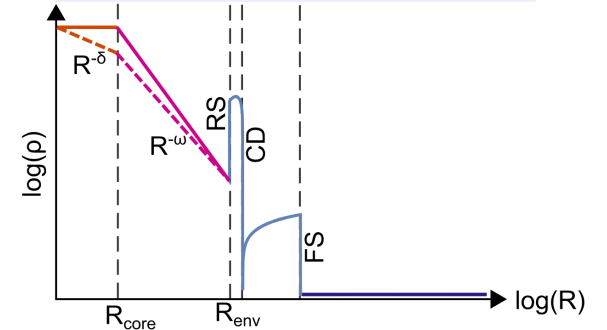
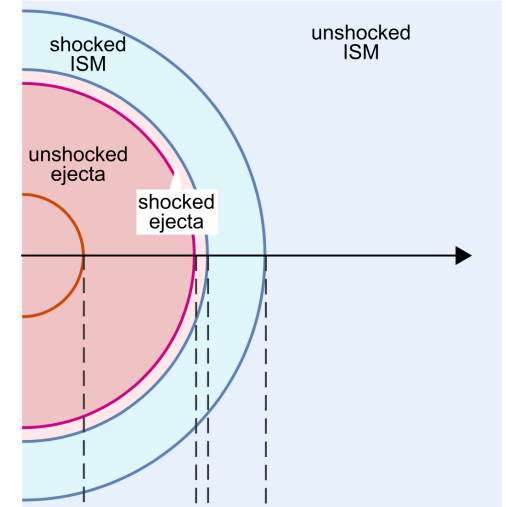
Typical models assume a **core** with a shallow radial profile $\propto r^{-\delta}$ (with $\delta < 3$), plus an **envelope** with a steep power-law one $\propto r^{-\omega}$ (with $\omega > 5$),

$$\rho_{\text{ej}}(r, t) = \begin{cases} A (v_t/r)^\delta / t^{3-\delta}, & \text{if } r < v_t t, \\ A (v_t/r)^\omega t^{\omega-3}, & \text{if } v_t t \leq r < R_{\text{RS}} \end{cases} \quad \begin{cases} v_t = \sqrt{\frac{2(5-\delta)(\omega-5)}{(3-\delta)(\omega-3)} \frac{E_{\text{sn}}}{M_{\text{ej}}}} \\ A = \frac{(5-\delta)(\omega-5)}{2\pi(\omega-\delta)} \frac{E_{\text{sn}}}{v_t^5} \end{cases}$$



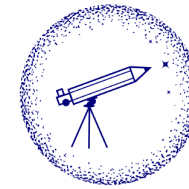
MULTIMESSENGER ASTROPHYSICS

COSMIC RAYS - COMPACT OBJECTS - RELATIVISTIC ENVIRONMENTS
© THE INSTITUTE OF SPACE SCIENCES (ICE, CSIC) SINCE 2006



PWN behavior very sensitive to RS location

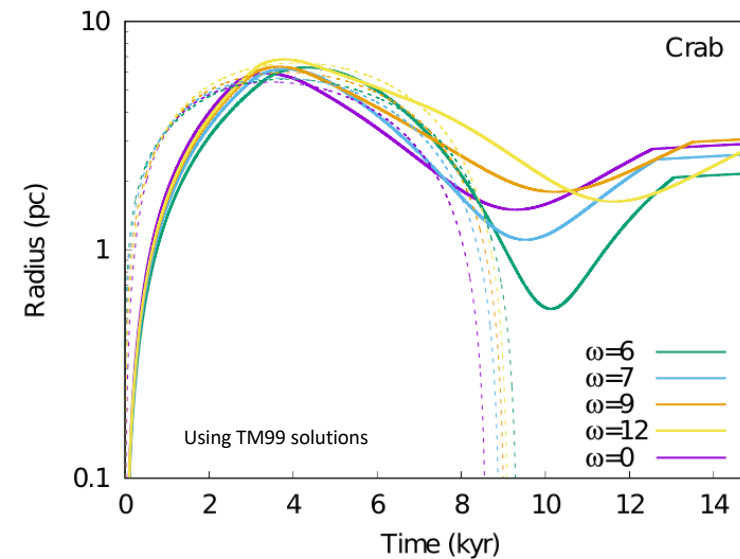
Bandiera, Bucciantini, Martin, Olmi & Torres, MNRAS 2020, 2021



**MULTIMESSENGER
ASTROPHYSICS**

COSMIC RAYS - COMPACT OBJECTS - RELATIVISTIC ENVIRONMENTS
© THE INSTITUTE OF SPACE SCIENCES (ICE, CSIC) SINCE 2006

Even small variations of the position and velocity of the RS at the onset of reverberation may produce large variations in the final compression factor of the PWN.



Shock positions

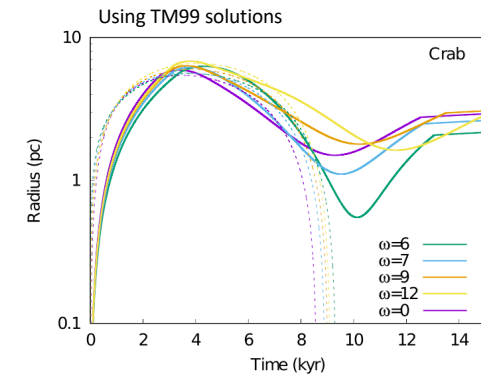


• Direct comparison of our formulae for the characteristic trajectories RS, CD, FS with those of [TM99](#) (only valid for $\delta = 0$).

Truelove J. K., McKee C. F., 1999, ApJS, 120, 299 (TM99)		ω	t	SUPPORTING FORMULAS
	$1.83t(1 + 3.26t^{3/2})^{-2/3}$	$\omega = 0$	$t < t_{st}$	$t_{st} = (2\omega/[5(\omega - 3)]\hat{A}^{-\omega/(\omega-3)}\sqrt{2.026})^{2\omega/[3(\omega-5)]}$ $\hat{A} = \{27l_{ed}^{(\omega-2)}/[4\pi\omega(\omega-3)\phi_{ed}](10[\omega-5]/[3(\omega-3)])^{(\omega-3)/2}\}^{1/\omega}$ $l_{ed} = \{1.39, 1.26, 1.21, 1.19, 1.17, 1.15, 1.14\}^*$
	$t(0.779 - 0.106t - 0.533\ln t)$	$\omega = 0$	$t \geq t_{st}$	
RS	$\hat{A}t^{(\omega-3)/\omega}$	$5 < \omega \leq 14$	$t \leq t_{core}$	$t_{core} = [27/(4\pi\omega[\omega-3]l_{ed}^2\phi_{ed})]^{1/3}\sqrt{3(\omega-3)/(10[\omega-5])}$ $\phi_{ed} = \{0.39, 0.47, 0.52, 0.55, 0.57, 0.6, 0.62\}^*$
	$t(\hat{A}t_{core}^{(\omega-3)/\omega}/l_{ed})$	$5 < \omega \leq 14$	$t_{core} < t \leq t_{st}$	
	$t[(\hat{A}t_{core}^{(\omega-3)/\omega})/(l_{ed}t_{core}) - a_{core}(t - t_{core}) + (3/(l_{ed}\omega)\hat{A}t_{core}^{[(\omega-3)/\omega]-1} - a_{core}t_{core})\ln(t/t_{core})]$	$5 < \omega \leq 14$	$t > t_{st}$	$a_{core} = \{0.112, 0.116, 0.139, 0.162, 0.192, 0.251, 0.277\}^*$
CD	—	—	—	—
FS	$2.01t(1 + 1.72t^{3/2})^{-2/3}$	$\omega = 0$	$t < t_{st}$	$(\hat{A}t_{st}^{(\omega-3)/\omega})^{5/2} + \sqrt{2.026}(t - t_{st})^{2/5}$
	$(1.42t - 0.254)^{2/5}$	$\omega = 0$	$t \geq t_{st}$	
	$\hat{A}t^{(\omega-3)/\omega}$	$5 < \omega \leq 14$	$t \leq t_{st}$	
		$5 < \omega < 14$	$t > t_{st}$	

Note that according to ω (the power law index of the ejecta profile) the time and extent of the compression varies a lot.

Not monotonous, not linear



*All the listed numerical values must be considered relative to the range $\omega = \{6, 7, 8, 9, 10, 12, 14\}$.

Shock positions



**MULTIMESSENGER
ASTROPHYSICS**

• Direct comparison of our formulae for the characteristic trajectories RS, CD, FS with those of [TM99](#) (only valid for $\delta = 0$).

Truelove J. K., McKee C. F., 1999, ApJS, 120, 299 (TM99)		ω	t	SUPPORTING FORMULAS
	$1.83t(1 + 3.26t^{3/2})^{-2/3}$	$\omega = 0$	$t < t_{st}$	$t_{st} = (2\omega/[5(\omega - 3)]\hat{A}^{-\omega/(\omega-3)}\sqrt{2.026})^{2\omega/[3(\omega-5)]}$
	$t(0.779 - 0.106t - 0.533\ln t)$	$\omega = 0$	$t \geq t_{st}$	$\hat{A} = \{27l_{ed}^{(\omega-2)}/[4\pi\omega(\omega-3)\phi_{ed}](10[\omega-5]/[3(\omega-3)])^{(\omega-3)/2}\}^{1/\omega}$
				$l_{ed} = \{1.39, 1.26, 1.21, 1.19, 1.17, 1.15, 1.14\}^*$
RS	$\hat{A}t^{(\omega-3)/\omega}$	$5 < \omega \leq 14$	$t \leq t_{core}$	$t_{core} = [27/(4\pi\omega[\omega-3]l_{ed}^2\phi_{ed})]^{1/3}\sqrt{3(\omega-3)/(10[\omega-5])}$
	$t(\hat{A}t_{core}^{(\omega-3)/\omega}/l_{ed})$	$5 < \omega \leq 14$	$t_{core} < t \leq t_{st}$	$\phi_{ed} = \{0.39, 0.47, 0.52, 0.55, 0.57, 0.6, 0.62\}^*$
	$t[(\hat{A}t_{core}^{(\omega-3)/\omega})/(l_{ed}t_{core}) - a_{core}(t - t_{core}) +$ $-(3/(l_{ed}\omega)\hat{A}t_{core}^{[(\omega-3)/\omega]-1} - a_{core}t_{core})\ln(t/t_{core})]$	$5 < \omega \leq 14$	$t > t_{st}$	$a_{core} = \{0.112, 0.116, 0.139, 0.162, 0.192, 0.251, 0.277\}^*$
CD	—	—	—	—
FS	$2.01t(1 + 1.72t^{3/2})^{-2/3}$	$\omega = 0$	$t < t_{st}$	
	$(1.42t - 0.254)^{2/5}$	$\omega = 0$	$t \geq t_{st}$	
	$\hat{A}t^{(\omega-3)/\omega}$	$5 < \omega \leq 14$	$t \leq t_{st}$	
	$(\hat{A}t_{st}^{(\omega-3)/\omega})^{5/2} + \sqrt{2.026}(t - t_{st})^{2/5}$	$5 < \omega < 14$	$t > t_{st}$	

We did 1D Lagrangian simulations for a large number of PWN, with different energetics, ω and δ parameters, and different characteristic values of the system and directly measured the shock positions.

Then fitted with functions providing much better than 1% accuracy, and compared the results with TM99 solutions.

*All the listed numerical values must be considered relative to the range $\omega = \{6, 7, 8, 9, 10, 12, 14\}$.

Shock positions



**MULTIMESSENGER
ASTROPHYSICS**

• Direct comparison of our formulae for the characteristic trajectories RS, CD, FS with those of [TM99](#) (only valid for $\delta = 0$).

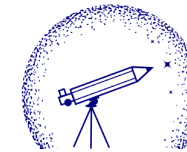
Truelove J. K., McKee C. F., 1999, ApJS, 120, 299 (TM99)		ω	t	SUPPORTING FORMULAS
	$1.83t(1 + 3.26t^{3/2})^{-2/3}$	$\omega = 0$	$t < t_{\text{st}}$	$t_{\text{st}} = (2\omega/[5(\omega - 3)]\hat{A}^{-\omega/(\omega-3)}\sqrt{2.026})^{2\omega/[3(\omega-5)]}$ $\hat{A} = \{27l_{\text{ed}}^{(\omega-2)}/[4\pi\omega(\omega-3)\phi_{\text{ed}}](10[\omega-5]/[3(\omega-3)])^{(\omega-3)/2}\}^{1/\omega}$ $l_{\text{ed}} = \{1.39, 1.26, 1.21, 1.19, 1.17, 1.15, 1.14\}^*$
	$t(0.779 - 0.106t - 0.533\ln t)$	$\omega = 0$	$t \geq t_{\text{st}}$	
RS	$\hat{A}t^{(\omega-3)/\omega}$	$5 < \omega \leq 14$	$t \leq t_{\text{core}}$	$t_{\text{core}} = [27/(4\pi\omega[\omega-3]l_{\text{ed}}^2\phi_{\text{ed}})]^{1/3}\sqrt{3(\omega-3)/(10[\omega-5])}$ $\phi_{\text{ed}} = \{0.39, 0.47, 0.52, 0.55, 0.57, 0.6, 0.62\}^*$
	$t(\hat{A}t_{\text{core}}^{(\omega-3)/\omega}/l_{\text{ed}})$	$5 < \omega \leq 14$	$t_{\text{core}} < t \leq t_{\text{st}}$	
	$t[(\hat{A}t_{\text{core}}^{(\omega-3)/\omega})/(l_{\text{ed}}t_{\text{core}}) - a_{\text{core}}(t - t_{\text{core}}) + (3/(l_{\text{ed}}\omega)\hat{A}t_{\text{core}}^{[(\omega-3)/\omega]-1} - a_{\text{core}}t_{\text{core}})\ln(t/t_{\text{core}})]$	$5 < \omega \leq 14$	$t > t_{\text{st}}$	$a_{\text{core}} = \{0.112, 0.116, 0.139, 0.162, 0.192, 0.251, 0.277\}^*$
CD	—	—	—	—
FS	$2.01t(1 + 1.72t^{3/2})^{-2/3}$	$\omega = 0$	$t < t_{\text{st}}$	
	$(1.42t - 0.254)^{2/5}$	$\omega = 0$	$t \geq t_{\text{st}}$	
	$\hat{A}t^{(\omega-3)/\omega}$	$5 < \omega \leq 14$	$t \leq t_{\text{st}}$	
	$(\hat{A}t_{\text{st}}^{(\omega-3)/\omega})^{5/2} + \sqrt{2.026}(t - t_{\text{st}})^{2/5}$	$5 < \omega < 14$	$t > t_{\text{st}}$	
Bandiera, Bucciantini, Martin, Olmi & DFT, MNRAS 2021		ω	t	SUPPORTING FORMULAS
RS	$\mathcal{R}(x) \times \mathcal{F}(\omega)$	$\omega \geq 6$	$t_{\text{core}} < t \leq t_{\text{implo}}$	$x = t/t_{\text{implo}}(\omega, \delta)$ $t_{\text{implo}} = 2.399 + \{(0.1006\Omega)^2 + [(-0.06494 + 0.7063\Omega)/(1 + 1/\Omega^2)]^2\}^{0.5}$ $\Omega = 1/(\omega - 5)$
				$\mathcal{R}(x) = [x^{1.5551}(1-x)^{0.68236}][0.01961 + 0.5093x + 0.1874x^2]^{-1}$ $\mathcal{F}(\omega) = 1 + \{0.02171[\Omega/0.3338 - 1]\}[1 + [\Omega/0.3338]^{-2.778}]^{-1}$
CD	$\tilde{a}(\omega)t^{(\omega-3)/\omega}/[1 + b_{\text{CD}}(\omega)t^{c_{\text{CD}}(\omega)}]$	$\omega \geq 6$	$t_{\text{core,CD}} < t \leq t_{\text{implo}}$	$\tilde{a}(\omega) = (1.141 + 1.806\omega)(7.636 + \omega)^{-1}$ $b_{\text{CD}} = -1.051 - 0.1961\tilde{a}(\omega)$ $c_{\text{CD}} = -(5.561 + 0.6741\omega)(\omega - 4.826)^{-1}$
FS	$\xi_0(t + 1.94)^{2/5}/[1 + 0.672(1/t) + 0.00373(1/t)^2]$	$\omega \geq 6$	$t > t_{\text{core,FS}}$	$\xi_0 = 1.15169$ (from the standard Sedov solution)

*All the listed numerical values must be considered relative to the range $\omega = \{6, 7, 8, 9, 10, 12, 14\}$.

Valid for all ω larger than 6, all values of δ .

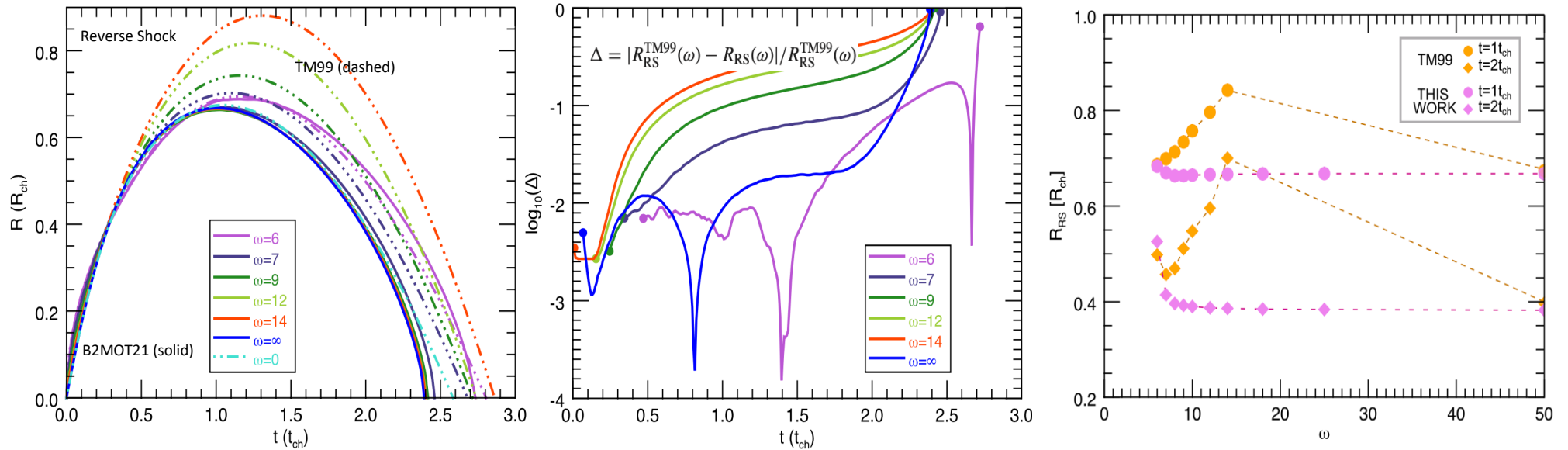
Shock positions inaccuracies can be large

Bandiera, Bucciantini, Martin, Olmi & DFT, MNRAS 2021



**MULTIMESSENGER
ASTROPHYSICS**

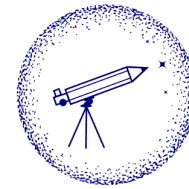
COSMIC RAYS - COMPACT OBJECTS - RELATIVISTIC ENVIRONMENTS



**The relative variation between models is typically of order of 10 to 30% per cent.
Impact of a 10% change in the compression is large and cannot be neglected!**

**Even larger relative differences closer to the implosion time,
of the order of 100 per cent!**

The TM99 solutions do not converge, for large ω values, to their asymptotic solution $\omega = 0$ ($\omega = \infty$ in our notation).



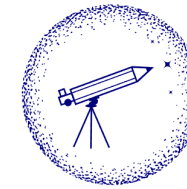
**MULTIMESSENGER
ASTROPHYSICS**

COSMIC RAYS - COMPACT OBJECTS - RELATIVISTIC ENVIRONMENTS

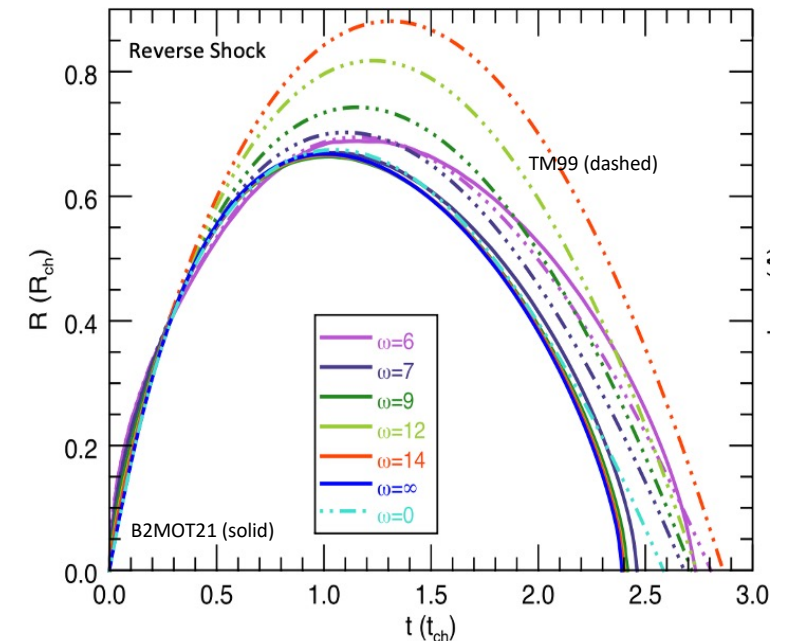
© THE INSTITUTE OF SPACE SCIENCES (ICE, CSIC) SINCE 2006

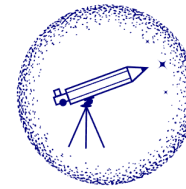
Age is not a good estimation of the PWN phase

Characteristic age of the SNR, not of the pulsar, as a marker of PWN stage



- $t_{\text{ch}} = E_{\text{sn}}^{-1/2} M_{\text{ej}}^{5/6} \rho^{-1/3}$,
- provides the typical time scale for the evolution of the SNR.
- Large variations of the implosion time only appear when drastically changing the structure of the ejecta core, being ~ 2.4 times the characteristic time of the SNR in many cases.
- $\sim 2.4 t_{\text{ch}}$ represents a theoretical maximum for the time the PWN can remain in free-expansion, as for typical PSR energy injection, the duration of the free-expansion phase we found to be no longer than about half of the implosion time.
- This clarifies why **the age of the pulsar may have no direct appeal in defining the phases, as for instance changes in the ejecta mass have an almost linear dependence on t_{ch} .**





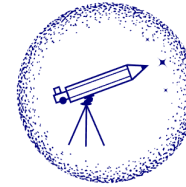
**MULTIMESSENGER
ASTROPHYSICS**

COSMIC RAYS - COMPACT OBJECTS - RELATIVISTIC ENVIRONMENTS

© THE INSTITUTE OF SPACE SCIENCES (ICE, CSIC) SINCE 2006

**Reverberation has its complexities,
disregarding/ignoring them leads to unreliable estimates**

PWN 1-zone-models: literature either ignores reverberation at all, or treats it in simplified ways



**MULTIMESSENGER
ASTROPHYSICS**

COSMIC RAYS - COMPACT OBJECTS - RELATIVISTIC ENVIRONMENTS
© THE INSTITUTE OF SPACE SCIENCES (ICE, CSIC) SINCE 2006

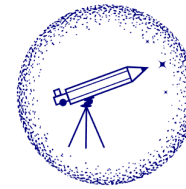
In the latter case, there are 3 main assumptions:

1. The PWN is a **uniform** (one-zone) bubble of particles and field
2. The shell at the PWN boundary is **thin** ($R_{\text{shell}} \sim R_{\text{pwn}} ; \Delta R_{\text{shell}} \ll R_{\text{pwn}}$)
3. The **pressure outside** the PWN is **equal to or a constant fraction of** the pressure at the FS in the **Sedov** solution

$$P_{\text{Sedov}} = 0.1592 \left(\frac{t}{t_{\text{ch}}} \right)^{-6/5} \frac{\rho_{\text{ISM}} E_{\text{sn}}}{M_{\text{ej}}}$$

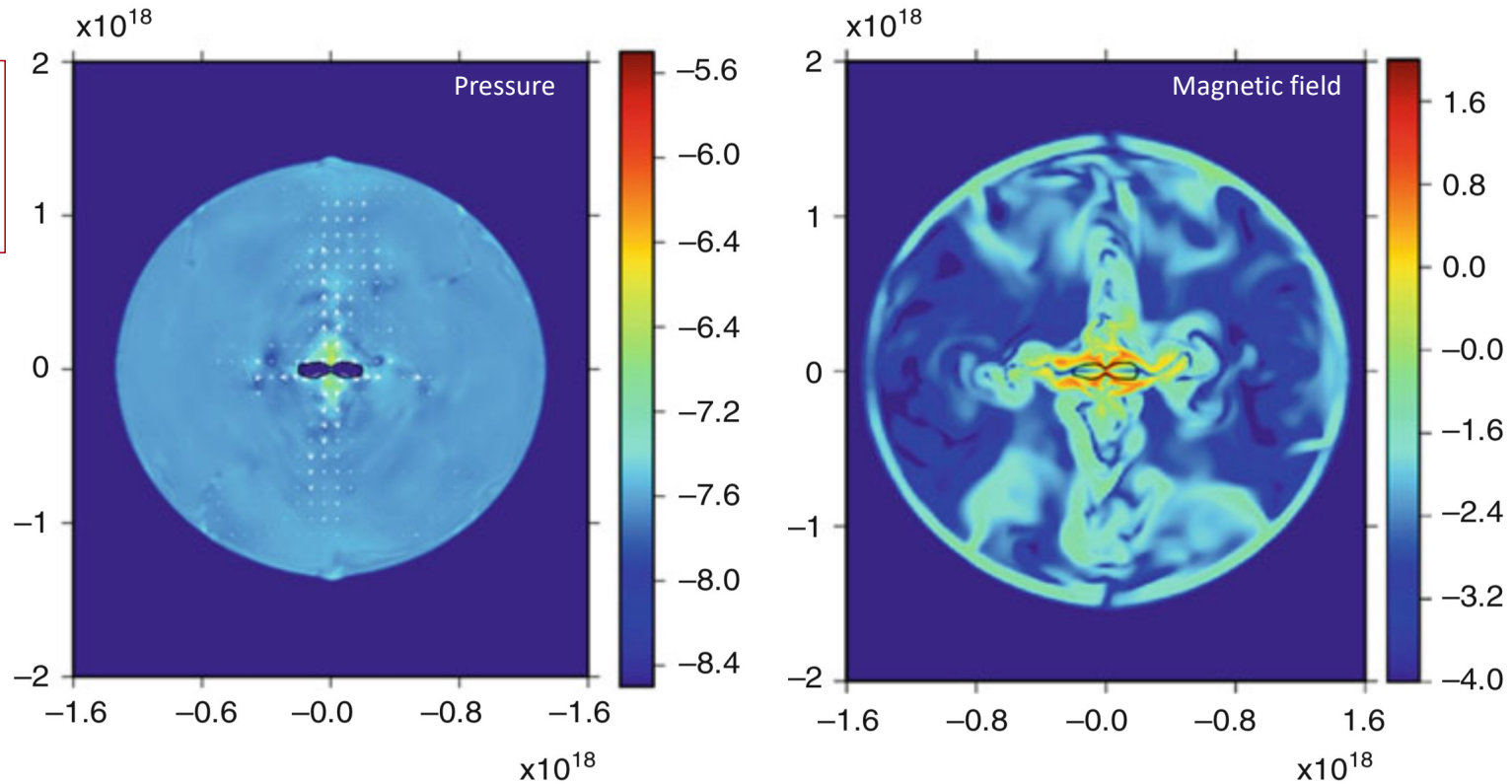
[Gelfand et al. 2009 - Fang & Zhang 2010 - Tanaka & Takahara 2010 - Martin et al. 2012 - Tanaka & Takahara 2013 - Vorster et al. 2013 - Torres et al. 2013-2019 - Gelfand et al. 2015-2017 - Bandiera et al. 2021 - Fiori et al. 2022]

First assumption... roughly ok, according to 3D MHD models



Porth et al. 2014
Crab @ ~50 years

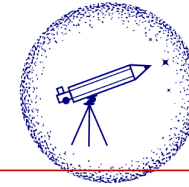
Olmi et al. 2019
Crab @ ~250 years



The PWN seems to be a rather uniform (one-zone) bubble of particles and field (but see IXPE).

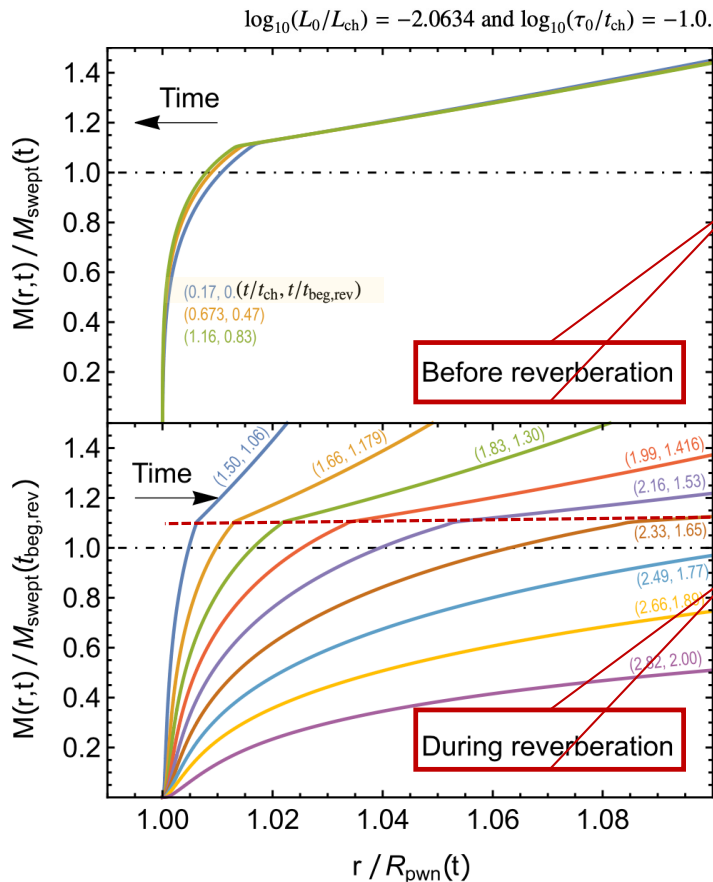
The thin-shell is not thin in reverberation

Bandiera, Bucciantini, Martin, Olmi & DFT, MNRAS 2023a



**MULTIMESSENGER
ASTROPHYSICS**

COSMIC RAYS - COMPACT OBJECTS - RELATIVISTIC ENVIRONMENTS
© THE INSTITUTE OF SPACE SCIENCES (ICE, CSIC) SINCE 2006



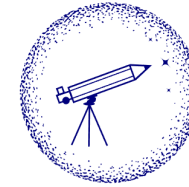
- For a scaled radius ranging between 1 and 1.02, the profiles are related to the density profile inside the shell.
- They are superimposed, meaning that the density preserves its profile, apart from a slight decrease with time of the shell relative width.
- The sharp break in the profiles (reflecting a density jump) indicates the position of the shock at the outer boundary of the shell;
- The scaled mass higher than unity means that the real swept-up mass is that within the outer boundary of the shell, rather than within $R_{pwn}(t)$.

- After $t_{beg,rev}$ the mass within the shell, now scaled with the swept-up mass at $t_{beg,rev}$, does not change with time: note the constancy of the vertical coordinate of the break
- The relative width of the shell increases with time, partly reflecting its physical broadening, and partly as a consequence PWN decreasing of its size.

This figure justifies the assumption of a **fixed shell mass during reverberation** and that when the PWN has been compressed, the **needed conditions for treating the shell as a thin-shell are no longer valid.**

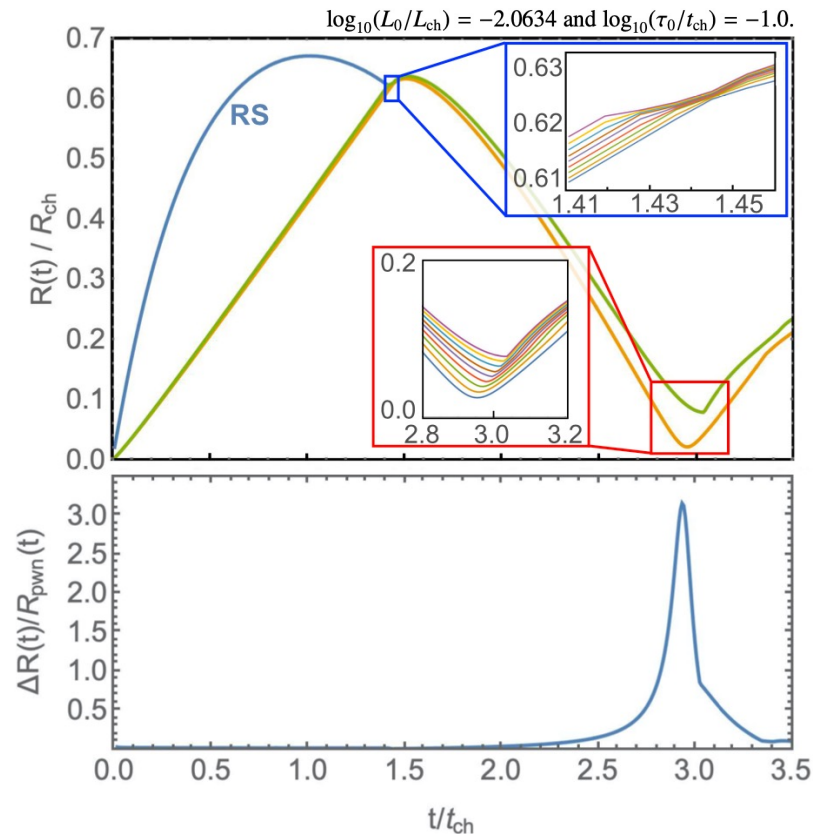
The thin-shell is not thin in reverberation

Bandiera, Bucciantini, Martin, Olmi & DFT, MNRAS 2023a



**MULTIMESSENGER
ASTROPHYSICS**

COSMIC RAYS - COMPACT OBJECTS - RELATIVISTIC ENVIRONMENTS
© THE INSTITUTE OF SPACE SCIENCES (ICE, CSIC) SINCE 2006



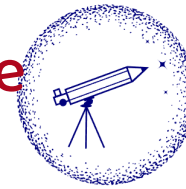
For $t < t_{\text{beg,rev}}$ the shell boundaries are very close each other, meaning that the thin-shell approximation is well satisfied.

But especially close to the maximum compression, the shell boundaries separate, and the combination of a higher shell thickness and a smaller shell size implies that a thin-shell approach is no longer justified.

During the reverberation phase, the outer edge of the shell is defined by the mass collected before $t_{\text{beg,rev}}$ and one may clearly see that the shell becomes thicker, and as the PWN starts to contract the shell inflates progressively

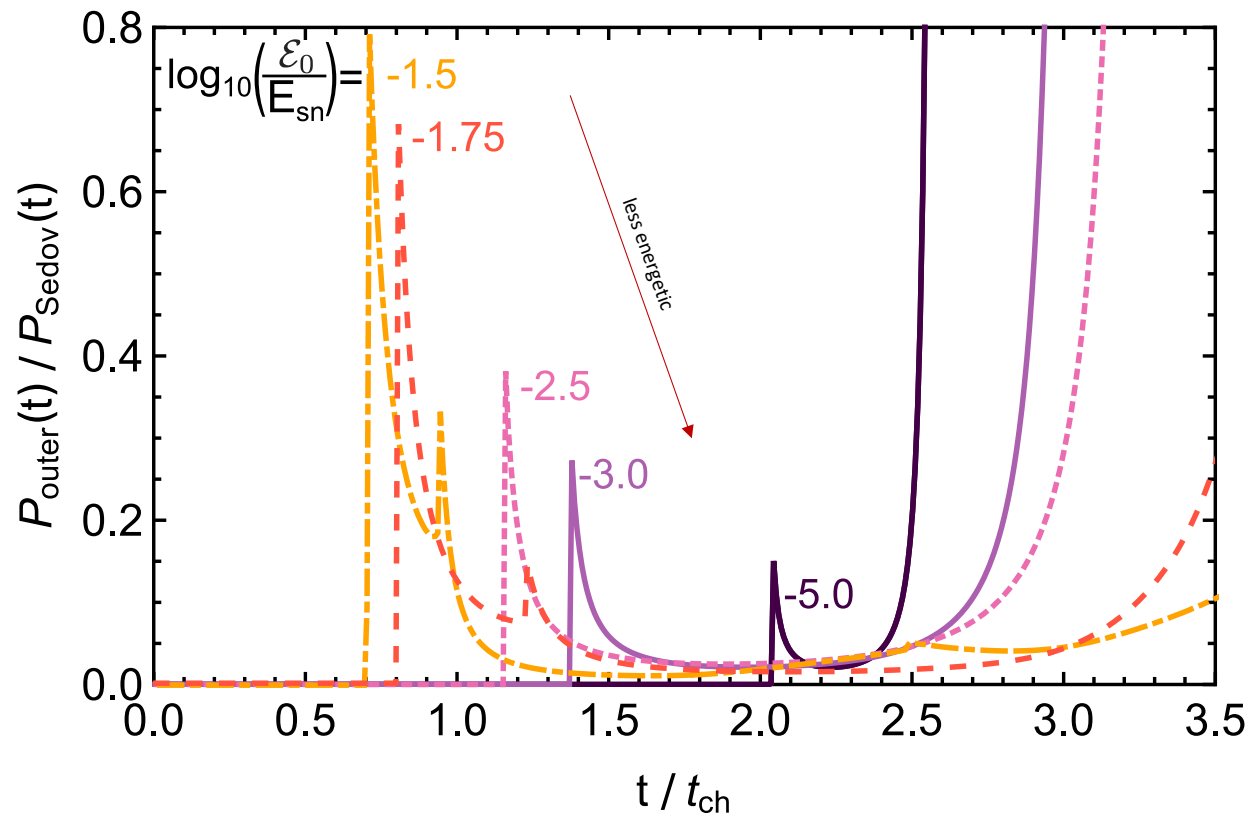
The outer pressure is not a constant nor Sedov like

Bandiera, Bucciantini, Martin, Olmi & DFT, MNRAS 2023a



**MULTIMESSENGER
ASTROPHYSICS**

COSMIC RAYS - COMPACT OBJECTS - RELATIVISTIC ENVIRONMENTS
© THE INSTITUTE OF SPACE SCIENCES (ICE, CSIC) SINCE 2006

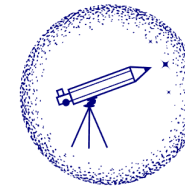


$\varepsilon_0 = L_0 \tau_0$ is the PWN energetics

$$P_{\text{Sedov}}(t) = 0.0489 \left(\frac{t}{t_{\text{ch}}} \right)^{-6/5} \frac{\rho_0 E_{\text{sn}}}{M_{\text{ej}}}$$

For a large part of the evolution P_{outer} is smaller than the Sedov pressure, and is different from a constant.

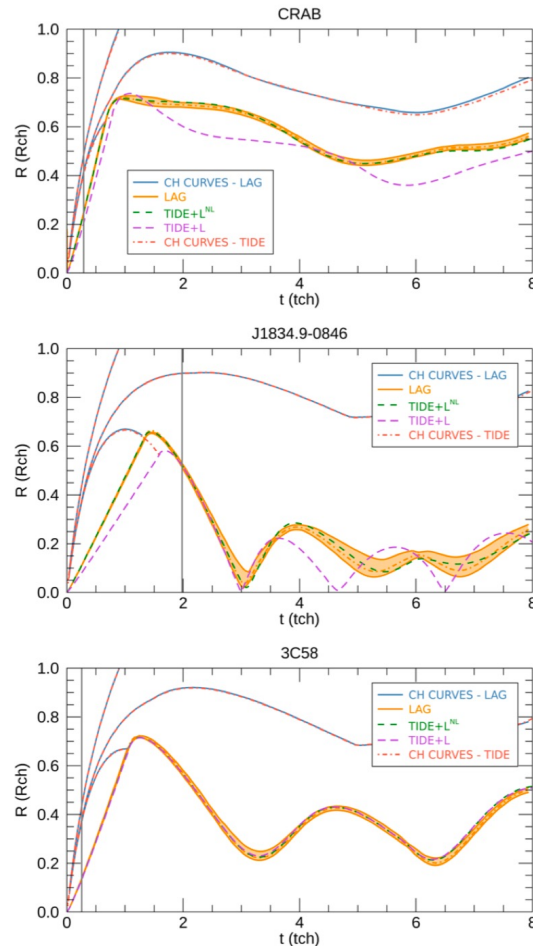
Modeling middle age systems



Bandiera, Bucciantini, Martin, Olmi & DFT, MNRAS 2023b

TIDE+L

Hybrid radiative – HD model



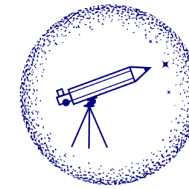
- Radiative model until reverberation, with dynamics incorporated
 - then use this stage just before reverberation as input for a...
- Lagrangian model thereafter,
 - But with radiation incorporated
- Correctly converges to the Lagrangian model all along when no losses are considered.
- Correctly matches at the interface between the two approaches.
- Relative fast for reasonable computational grid (few minutes per PWN).
- Can go to whatever age in a safe manner.

(State-of-the-art Radiative PWN code: correct shock positions, radiative, full ODEs, time-energy-dependent, Lagrangian after Reverberation)

Of course, recall, all of this is 3D in nature. Still an approximation!

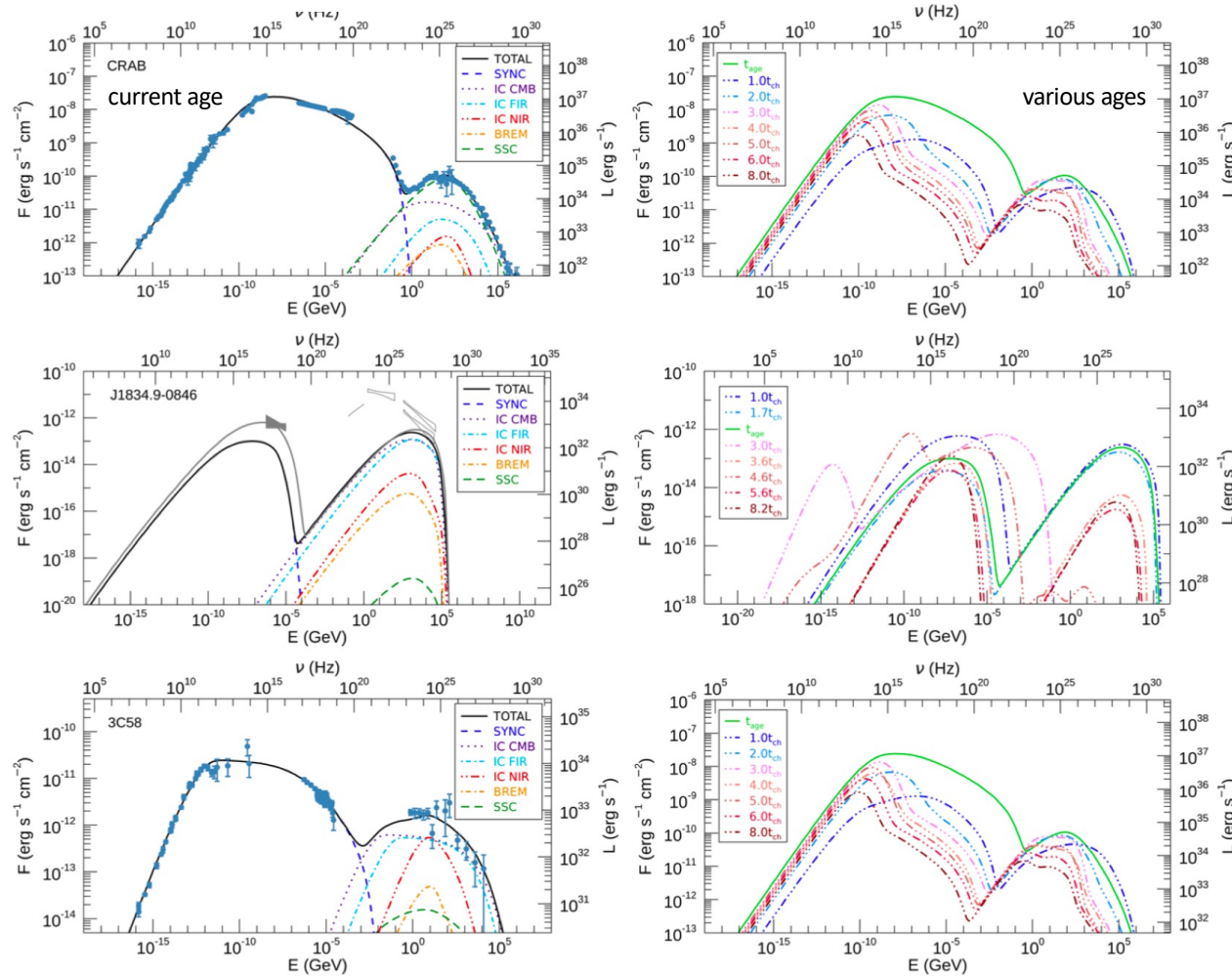
How to model middle age systems? Spectra

Bandiera, Bucciantini, Martin, Olmi & DFT, MNRAS 2023b



**MULTIMESSENGER
ASTROPHYSICS**

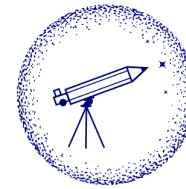
COSMIC RAYS - COMPACT OBJECTS - RELATIVISTIC ENVIRONMENTS
© THE INSTITUTE OF SPACE SCIENCES (ICE, CSIC) SINCE 2006



Significant spectral variability as time goes by

Superefficiency

Population analysis finally possible (ongoing research)



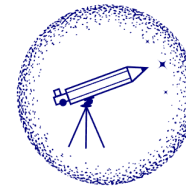
**MULTIMESSENGER
ASTROPHYSICS**

COSMIC RAYS - COMPACT OBJECTS - RELATIVISTIC ENVIRONMENTS

© THE INSTITUTE OF SPACE SCIENCES (ICE, CSIC) SINCE 2006

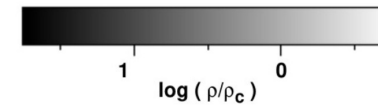
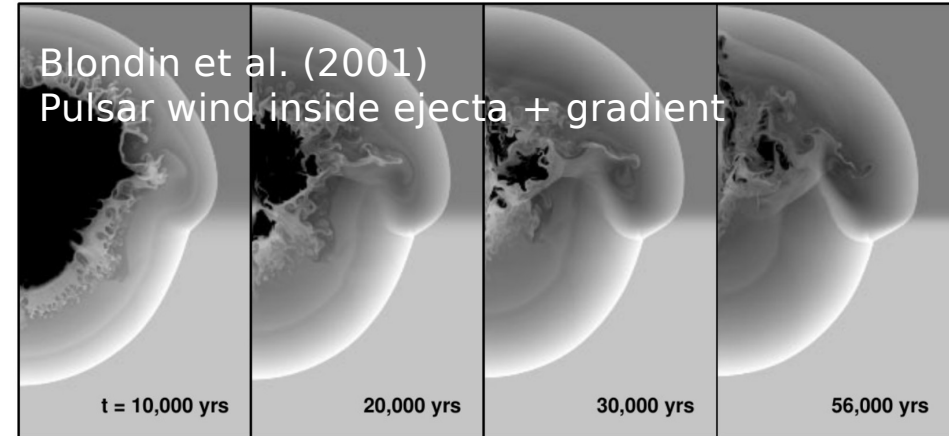
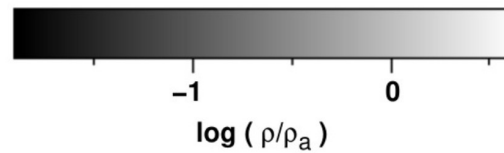
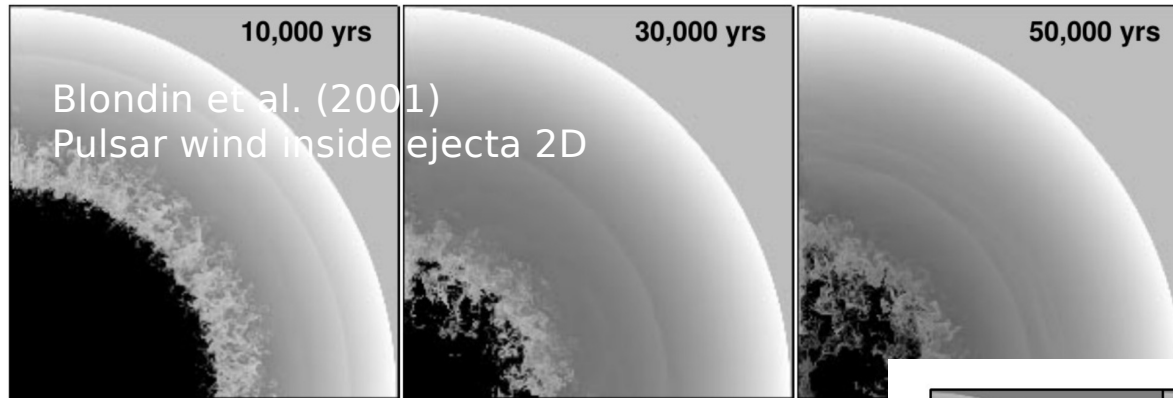
**PWN morphology very strongly depends on the environment,
and the latter is not mainly determined by the ISM**

HD/MHD models of PWN

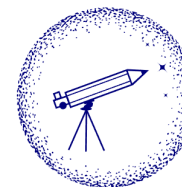


**MULTIMESSENGER
ASTROPHYSICS**

COSMIC RAYS - COMPACT OBJECTS - RELATIVISTIC ENVIRONMENTS
© THE INSTITUTE OF SPACE SCIENCES (ICE, CSIC) SINCE 2006

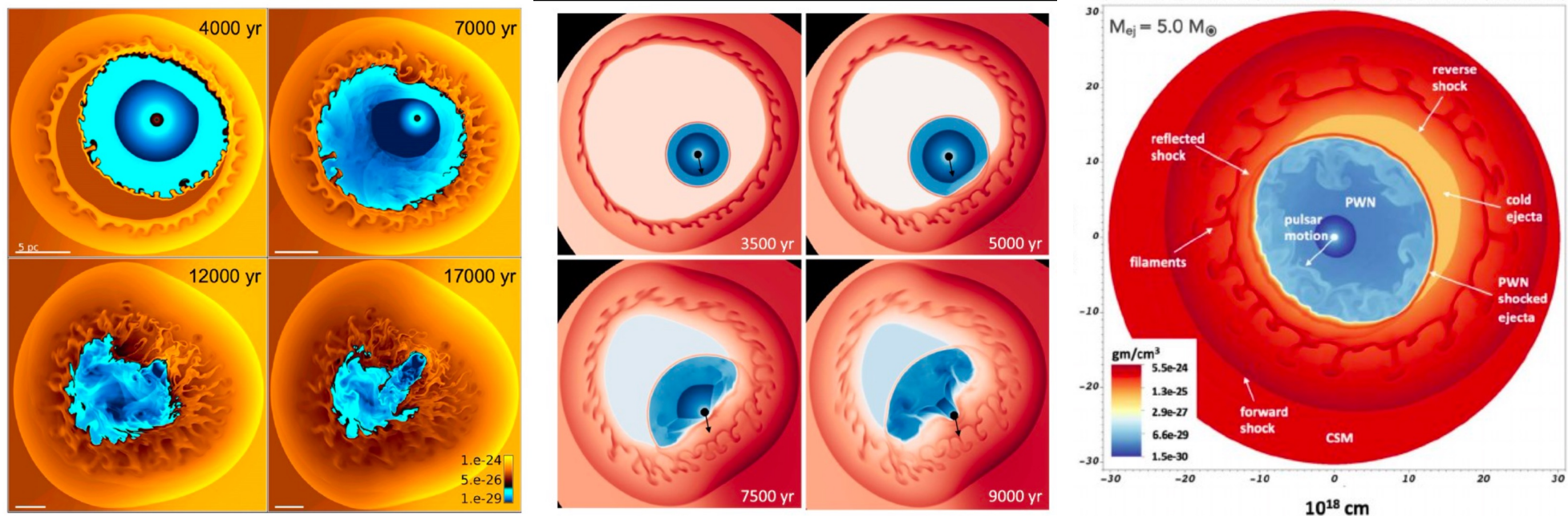


Previously: hydrodynamical models of PWN



**MULTIMESSENGER
ASTROPHYSICS**

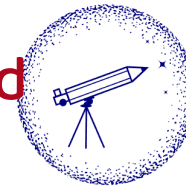
COSMIC RAYS - COMPACT OBJECTS - RELATIVISTIC ENVIRONMENTS
© THE INSTITUTE OF SPACE SCIENCES (ICE, CSIC) SINCE 2006



Temim et al. (2015, 2017a,b, 2022)

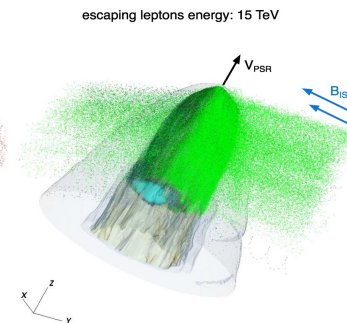
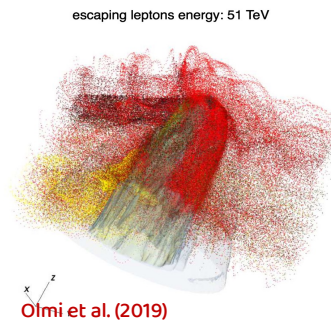
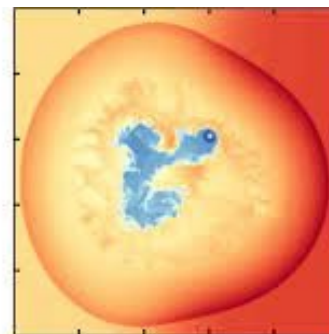
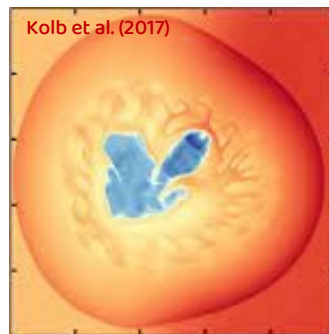
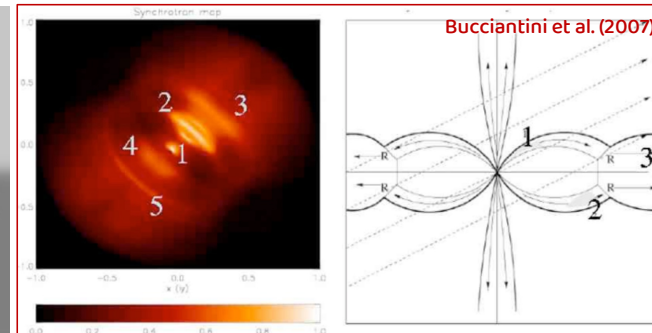
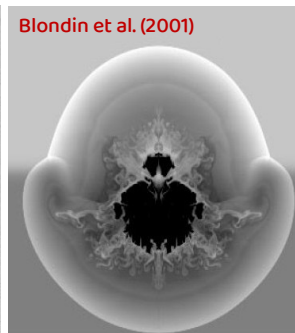
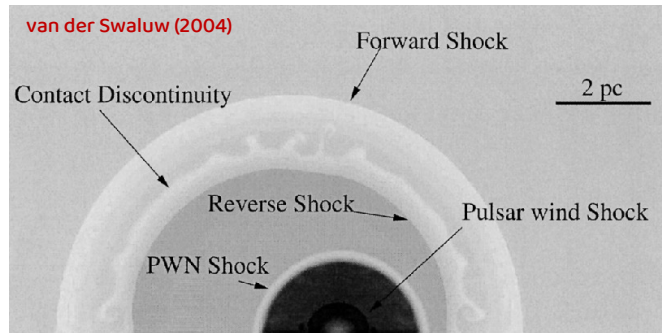
Pulsar wind that is moving inside supernova ejecta and/or in a density gradient in the ISM

HD/MHD models of PWN: so far without stellar wind

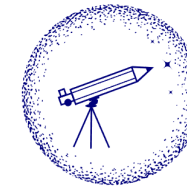


**MULTIMESSENGER
ASTROPHYSICS**

COSMIC RAYS - COMPACT OBJECTS - RELATIVISTIC ENVIRONMENTS
© THE INSTITUTE OF SPACE SCIENCES (ICE, CSIC) SINCE 2006

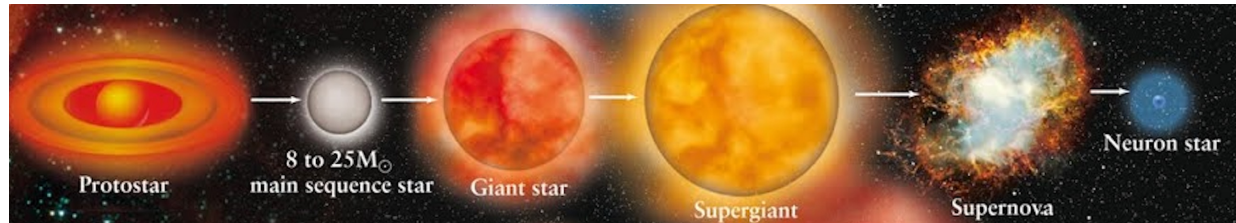


Stellar history + wind

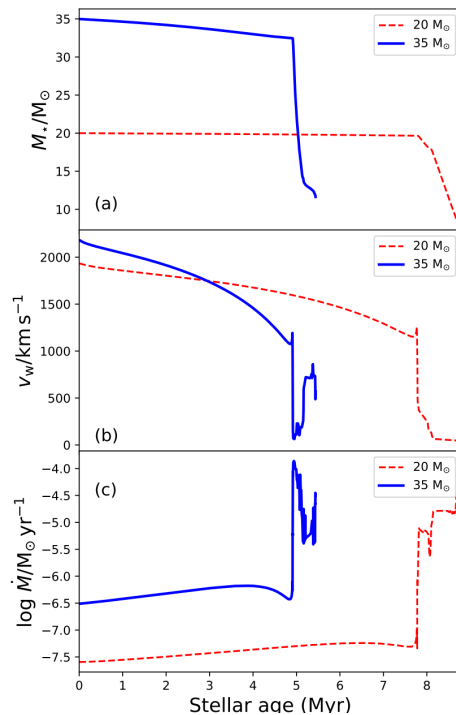


**MULTIMESSENGER
ASTROPHYSICS**

COSMIC RAYS - COMPACT OBJECTS - RELATIVISTIC ENVIRONMENTS
© THE INSTITUTE OF SPACE SCIENCES (ICE, CSIC) SINCE 2006



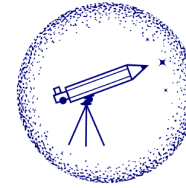
The interaction of the pulsar wind and SNR with the CSM generated by the supergiant and eventual phases of WR Or blue star has been essentially been neglected.



Runaway massive star die
in their own bow shock

The circumstellar medium of massive (runaway)
star is a governing parameter in the morphology,
distribution and mixing of materials in plerion

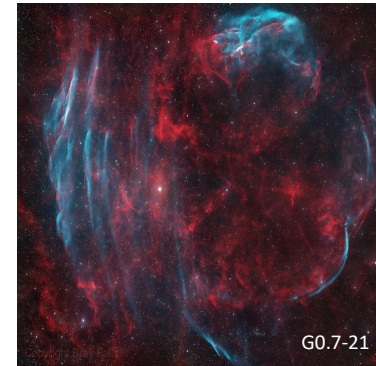
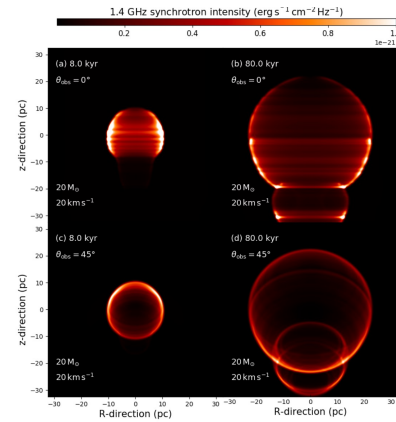
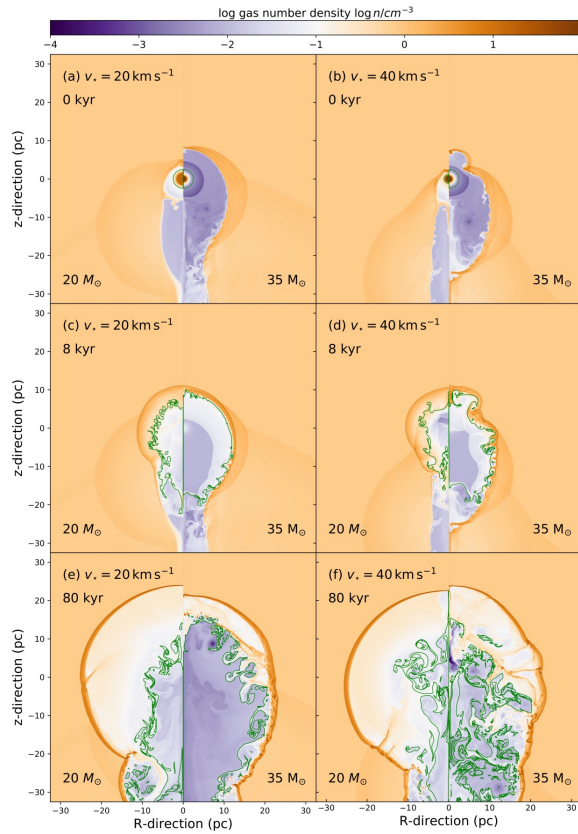
MHD num simulations of PWN/SNR w/CSM



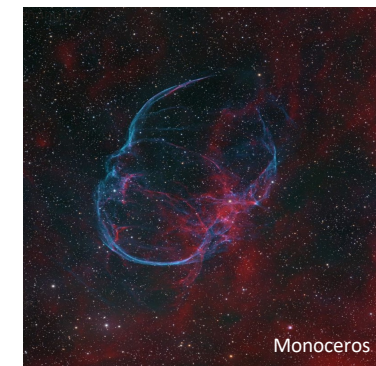
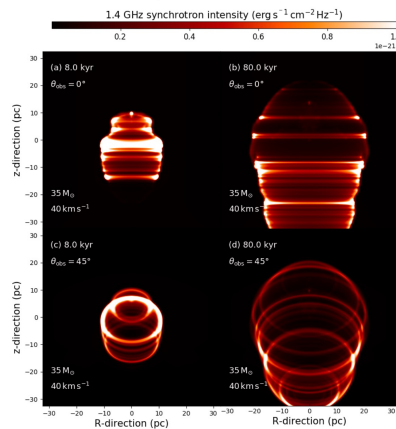
**MULTIMESSENGER
ASTROPHYSICS**

COSMIC RAYS - COMPACT OBJECTS - RELATIVISTIC ENVIRONMENTS
© THE INSTITUTE OF SPACE SCIENCES (ICE, CSIC) SINCE 2006

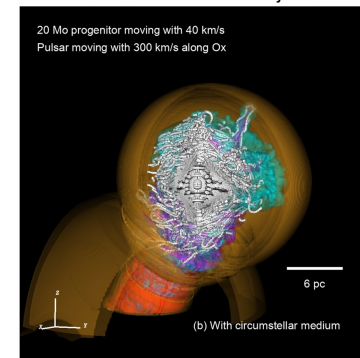
- D. Meyer, & D. F. Torres, Material mixing in pulsar wind nebulae of massive runaway stars. [A&A 2024](#)
- D. Meyer, Z. Meliani & D. F. Torres, Pulsar wind nebulae meeting the circumstellar medium of their progenitors [A&A 2024](#)
- D. Meyer et al. Supernova remnants of red supergiants: From barrels to loops, [A&A 2024](#)
- D. Meyer et al. On the plerionic rectangular supernova remnants of static progenitors, [A&A 2024](#)



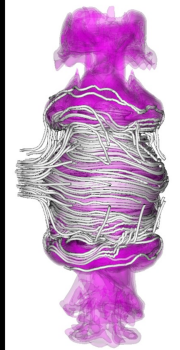
The interaction of the pulsar wind and SNR with the CSM generated by the supergiant and eventual phases of WR Or blue star has been so far neglected in literature

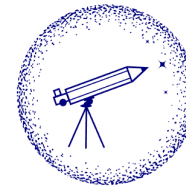


The 3D PWN Marenstrum Project



D. Meyer, D. F. Torres, & Z. Meliani 2025





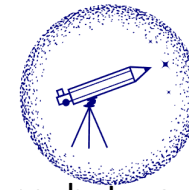
**MULTIMESSENGER
ASTROPHYSICS**

COSMIC RAYS - COMPACT OBJECTS - RELATIVISTIC ENVIRONMENTS

© THE INSTITUTE OF SPACE SCIENCES (ICE, CSIC) SINCE 2006

Concluding remarks

Conclusions



**MULTIMESSENGER
ASTROPHYSICS**

COSMIC RAYS - COMPACT OBJECTS - RELATIVISTIC ENVIRONMENTS
© THE INSTITUTE OF SPACE SCIENCES (ICE, CSIC) SINCE 2006

- Don't forget that it's more complicated than finding a pulsar with a high E_{sd} . Crab is young, but we all were.
- Go beyond Truelove and McKee, we now have well-behaving formulae mimicking directly HD simulations.
- Mixed one-zone/HD models solve the problems introduced by the pure thin-shell approximation in the treatment of the reverberation phase: they catch the global behavior and estimate the PWN compression
- First relatively consistent numerical passage through reverberation for a radiative/HD model (TIDE-L)
- Some PWNe can reduce themselves in size by more than two orders of magnitude, at least in the 1D representation.
 - Such systems with large compression $CF \gg 100$ are possible but rare, limited to the extremes of the known population of PWNe.
 - But reductions in size by a factor of a few-10x are quite common.
 - Superefficiency appears often at UV/optical, and less often in X-rays
- Understanding and correctly modelling reverberation is critical for population studies (e.g., how many PWN will we see in future surveys at different frequencies) and individual predictions / description of all middle-age systems
- The circumstellar (not just the interstellar) medium affects it all, opening a whole lot of new complexities into the problem.

Institute of
Space Sciences



Thank you

<https://sites.google.com/view/dft-research>

@dft_research

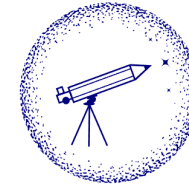


Institute of
Space Sciences



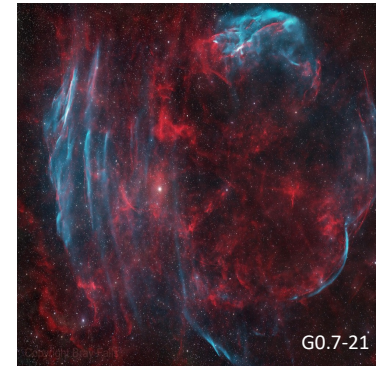
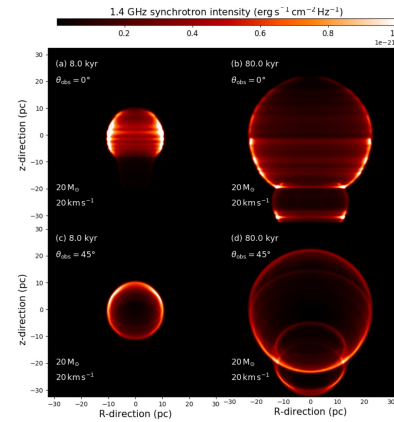
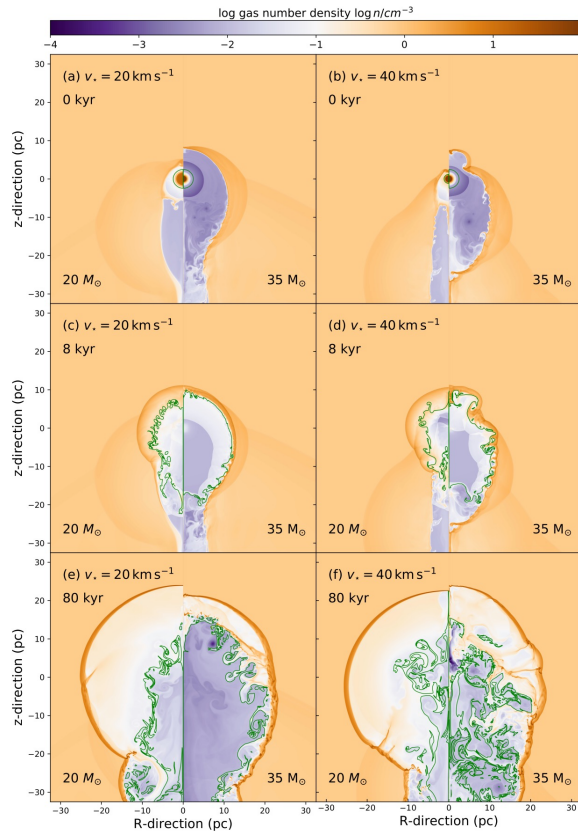
MHD num simulations of PWN/SNR w/CSM

- D. Meyer, & D. F. Torres, Material mixing in pulsar wind nebulae of massive runaway stars. [A&A 2024](#)
- D. Meyer, Z. Meliani & D. F. Torres, Pulsar wind nebulae meeting the circumstellar medium of their progenitors [A&A 2024](#)
- D. Meyer et al. Supernova remnants of red supergiants: From barrels to loops, [A&A 2024](#)
- D. Meyer et al. On the plerionic rectangular supernova remnants of static progenitors, [A&A 2024](#)

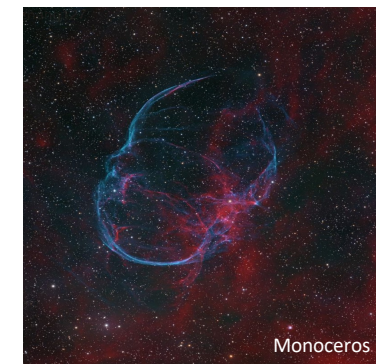
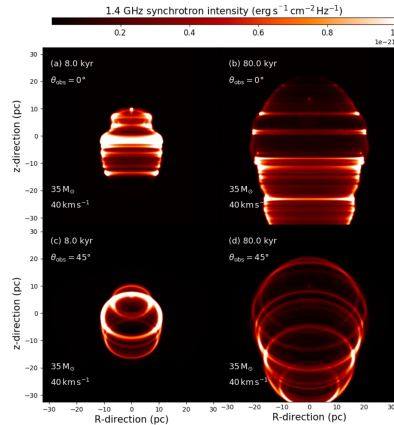


**MULTIMESSENGER
ASTROPHYSICS**

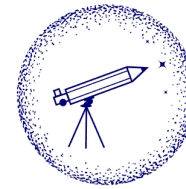
COSMIC RAYS - COMPACT OBJECTS - RELATIVISTIC ENVIRONMENTS
© THE INSTITUTE OF SPACE SCIENCES (ICE, CSIC) SINCE 2006



The interaction of the pulsar wind and SNR with the CSM generated by the supergiant and eventual phases of WR Or blue star has been so far neglected in literature

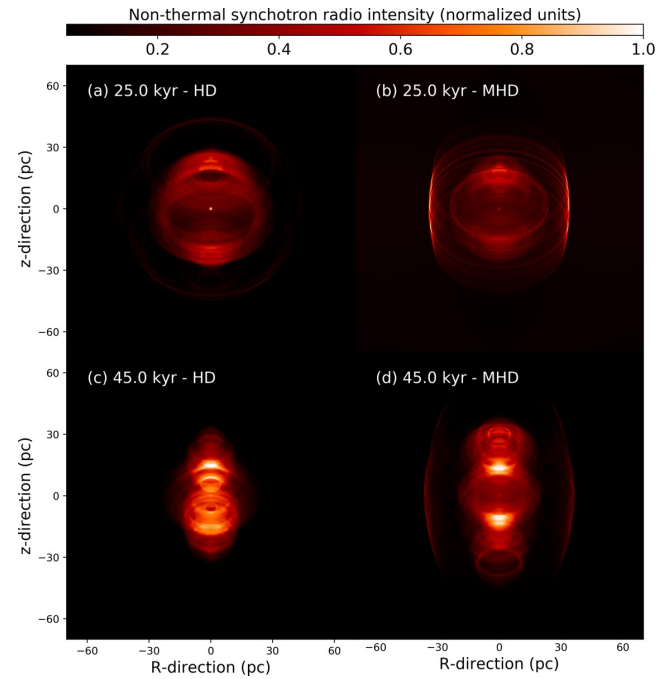
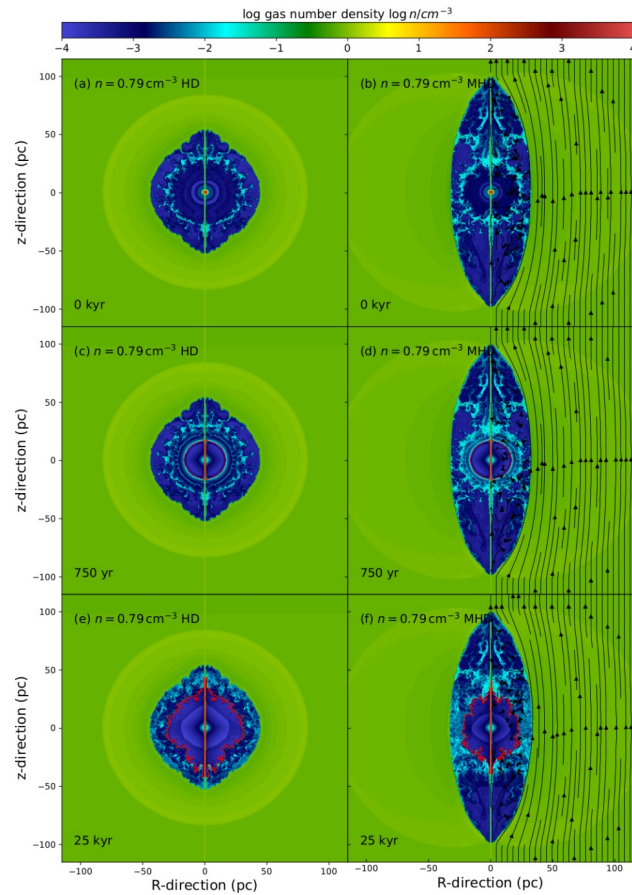


PWN in magnetised ISM



**MULTIMESSENGER
ASTROPHYSICS**

COSMIC RAYS - COMPACT OBJECTS - RELATIVISTIC ENVIRONMENTS
© THE INSTITUTE OF SPACE SCIENCES (ICE, CSIC) SINCE 2006



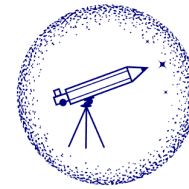
The magnetisation of the ISM changes the circumstellar medium of massive stars, and, consequently, their supernova remnant and PWN

Meyer et al. (2024)



The group's aim is doing frontier research in high-energy astrophysics from a multifrequency and multiparticle perspective.

Progenitor's stellar wind history induces asymmetric reverberation in PWN

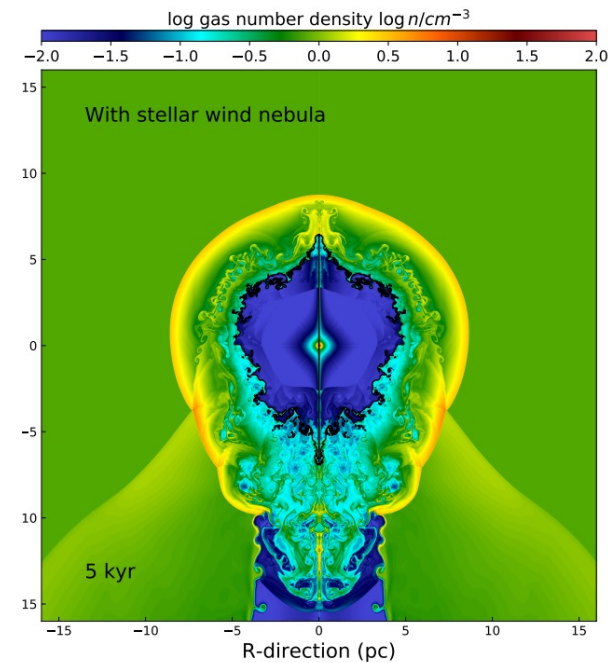
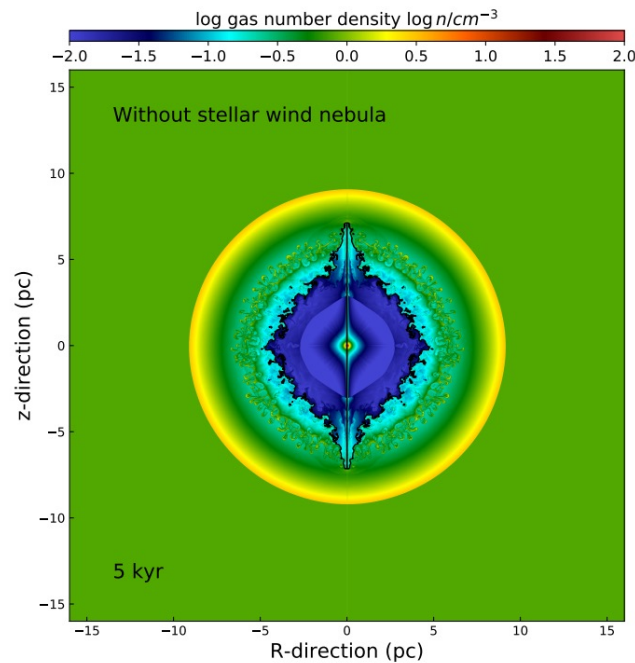


**MULTIMESSENGER
ASTROPHYSICS**

COSMIC RAYS - COMPACT OBJECTS - RELATIVISTIC ENVIRONMENTS
© THE INSTITUTE OF SPACE SCIENCES (ICE, CSIC) SINCE 2006



Wind nebulae
of SN progenitors



The interaction of the pulsar wind and SNR with the CSM generated by the supergiant and eventual phases of WR Or blue star has been essentially been neglected so far.

Meyer, Meliani, Torres (2024)